Appl Phys A (2013) 112:41–47
DOI 10.1007/s00339-012-7172-3

Applied Physics A
Materials Science & Processing

Electrode patterning on PEDOT:PSS thin films by pulsed ultraviolet laser for touch panel screens

Shih-Feng Tseng · Wen-Tse Hsiao · Kuo-Cheng Huang · Donyau Chiang

Received: 7 March 2011 / Published online: 6 September 2012

Abstract Laser dry etching by a laser driven direct writing apparatus has been extensively used for the micro- and nano-patterning on the solid surface. The purpose of this study is to pattern the PEDOT:PSS thin film coated on the soda-lime glass substrates by a nano-second pulsed ultraviolet laser processing system. The patterned PEDOT:PSS film structure provides the electrical isolation and prevents the electrical contact from each region for capacitive touch screens. The surface morphology, geometric dimension, and edge quality of ablated area after the variety of laser patternings were measured by a 3D confocal laser scanning microscope. After the single pulse laser irradiation, the ablation threshold of the PEDOT:PSS film conducted by the nano-second pulsed UV laser was determined to be 0.135 ± 0.003 J/cm^2. The single pulse laser interacted region and the ablated line depth increased with increasing the laser fluence. Moreover, the inner line width of ablated PEDOT:PSS films along the patterned line path increased with increasing the laser fluence but the shoulder width increased with decreasing fluence, respectively. The clean, smooth, and straight ablated edges were accomplished after the electrode patterning with the laser fluence of 1.7 J/cm^2 and 90 % overlapping rate.

1 Introduction

PEDOT:PSS [poly(3,4-ethylenedioxythiophene):poly(4-styrenesulfonate)] is one of transparent conductive polymer (TCP) thin films, which were applied as an conductor material in the touch panels, liquid crystal displays (LCDs), flexible electronics, thin film solar cells, light-emitting diodes (LEDs), and other optoelectronics products. Traditional electrode patterning techniques use the photoresistor lithography and chemical etching to form various patterns on the film surface. The electrode patterning process involves sequentially (a) photoresist coating, (b) soft bake, (c) exposure, (d) lithography, (e) hard bake, (f) etch, and (g) photoresist stripping [1–3]. These manufacturing equipments are expensive and require complicated steps in the fabrication process. Moreover, the PEDOT:PSS film surface is hydrophilic and easily peeled off after soaking in the liquid. And this caused the wet etching process to have a problem in patterning electrodes on the PEDOT:PSS film surface. Hence, laser dry etching is applied to fabricate an electrode structure on the PEDOT:PSS film surface. The dry patterning method has several advantages including high accuracy, high speed, high dimensional resolution, and flexible fabrication [4].

Some previous studies of laser patterning with different laser sources and processing methods on the film surface were discussed. Yu et al. [5] demonstrated a method to pattern the solution-processed oxide semiconductor thin films using a metal absorption layer by a spatially-modulated pulsed Nd:YAG laser. The patterned zinc-tin oxide (ZTO) structures at the micrometer scale with sharp edges were fabricated by a single pulse of 850 mJ. Chen et al. [6] developed a third harmonic Nd:YAG laser system to direct writing line patterns on ITO films and also used a laser beam shape technique to obtain top-hat intensity distribution to perform complex electrode patterning on ITO thin films deposited on glass and plastic substrates. These ablated electrodes were uniform and smooth, but some debris particles were found around the electrodes. Roch et al. [7] proposed

S.-F. Tseng (✉) · W.-T. Hsiao · K.-C. Huang · D. Chiang
Instrument Technology Research Center, National Applied Research Laboratories, Hsinchu 30076, Taiwan
e-mail: tsengsf@itrc.narl.org.tw
Fax: +886-3-5773947

a direct laser interference patterning on the hydrogen-free tetrahedral amorphous carbon (ta-C) thin film by a nano-second pulsed ultraviolet (UV) laser. A periodic line-like array with a grating period of 183 nm was fabricated on a 104 nm thick ta-C film by a UV-laser wavelength of 266 nm. Tseng et al. [2] used a Nd:YAG laser with wavelength of 1064 nm to scribe the ITO thin films deposited on three types of substrate materials, i.e. soda-lime glass, polycarbonate (PC), and cyclic-olefin-copolymer (COC) materials. The better edge quality of the scribed lines were obtained when the laser power was of 2.2 watts, the pulse repetition frequency of 100 kHz, and the exposure time extended from 30 μs to 60 μs. Shin et al. [8] reported that gold (Au) film grating patterns could be directly fabricated on glass substrates by an interfering the pulsed Nd:YAG laser with a wavelength of 1064 nm and a pulse width of 6 ns incident from the backside of the substrate. The interference profile was generated using a refracting prism made up of quartz. The patterned Au transmission grating with a minimum feature size of 1 μm could be produced by interference-driven periodic detachment. Lin et al. [9] utilized a UV laser with a wavelength of 355 nm to manufacture the metal electrode without a shadow mask for cholesteric liquid crystal displays (Ch-LCDs). The minimum ablated line was around 43 μm when the laser power and scan speed were 1.5 W and 200 mm/s, respectively. Hayden and Dalton [10] presented a quicker and simpler process to create micro-electrode arrays using a femtosecond laser for the lab-on-a-chip applications. No heat affect zone (HAZ) and a minimal amount of debris on the remaining gold/chrome microelectrodes were observed. Westin et al. [11] used a frequency-doubled Nd:YVO_4 laser of 532 nm wavelength scribing system to ablate Cu(In,Ga)Se_2 (CIGS) thin film without damaging the underlying molybdenum (Mo) layer for thin-film photovoltaic modules. The scribed lines were smooth, narrow, and straight. The resistivity of laser patterned contacts was found in the range of 0.4 $\Omega \cdot$ cm, which was higher than 0.1 $\Omega \cdot$ cm obtained from the mechanically patterned contacts.

In the present work, laser patterning was applied in the electrical isolation of PEDOT:PSS films using a single patterning step. A solid state diode pumped neodymium-doped yttrium vanadate (Nd:YVO_4) laser was used to pattern PEDOT:PSS films with thickness of 330 nm coated on soda-lime substrates. Moreover, a high speed galvanometer guided the laser beam to ablate directly PEDOT:PSS films. The processing parameters including the laser fluence, the pulse repetition frequency, and the scanning speed of galvanometers were used to ablate out the PEDOT:PSS films. The surface morphology, geometric dimension, and edge quality of ablated area after laser patterning were measured by a 3D confocal laser scanning microscope.

2 Experimental

2.1 Electrode patterning apparatus

A nano-second pulsed Nd:YVO_4 laser processing system (Coherent, Inc. model AVIA 355-14) with a wavelength of 355 nm was used to pattern isolation structures on the PEDOT:PSS film surface. The specifications of UV laser are following: the maximal power of 14 W at the pulse repetition frequency of 100 kHz, the transverse mode of TEM_{00}, and the maximal pulse repetition frequency of 300 kHz. The nominal values of the laser beam diameter at the exit port and average spot size are approximately 3.5 mm and 30 μm, respectively. Laser beam deflection was achieved using a galvanometer system (Raylase AG model SS-15) with a focus shifter. The focus shifting module consists of the moving lens and the focusing lens that can use to adjust the focus range in Z-direction from $+15$ mm to -15 mm, and the beam expander factor is 2 times. Moreover, the beam was focused onto the film surface through a telecentric lens of 110 mm focal length with a field size of 40 mm $\times$ 40 mm. To fabricate the isolated electrode structures on the PEDOT:PSS film surface, the beam is deflected continuously by two mirrors of a galvanometer scanner. The laser average output power, the pulse repetition frequency, and the scanning speed of galvanometer on the PEDOT:PSS/glass surface are controlled by the commercial software (Raylase AG weldMARK), which allows an automatic control during the laser patterning process.

2.2 Sample preparation

The PEDOT:PSS thin film, SiO_2 buffer layer stacked sequentially on the commercial soda lime glass was used as a sample. We denote the sample as a PEDOT:PSS/glass substrate through this article. The silicon dioxide buffer layer was first deposited on the substrate to enhance adhesion between the PEDOT:PSS film and substrate. And then, the PEDOT:PSS thin film was coated on the buffer material by a spin coating method. The PEDOT:PSS film and SiO_2 buffer layer were approximately 330 nm and 50 nm thick, respectively, measured by a scanning electron microscope (SEM, HITACHI model 4300). Figure 1 shows the SEM picture of cross-section view of stacked films coated on a glass substrate. A spectrophotometer (HITACHI model U-4001) was used to measure the transmittance and reflectance of the sample. The measured data is shown in Fig. 2. The light transmittance and reflectance values at 355 nm wavelength were approximately 74.4 % and 8.2 %, respectively. Therefore, the light absorptance value at 355 nm waveband was roughly 17.4 % for the PEDOT:PSS/glass substrate. The sheet resistance of PEDOT:PSS thin films was approximately 100 $\Omega/\square$ measured by a four-point probe instrument. Furthermore, the microhardness and reduced modulus

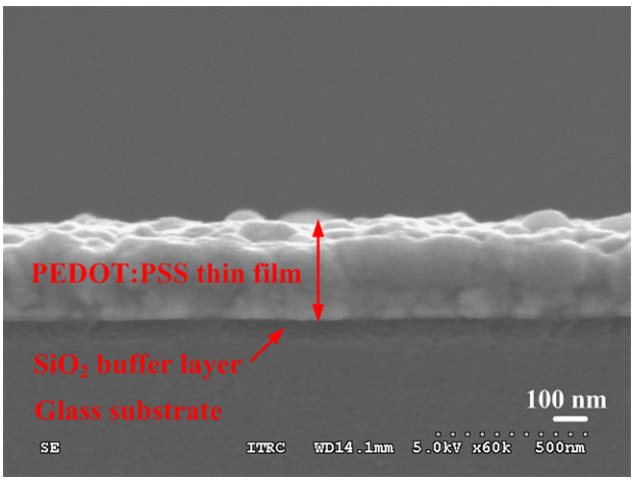

Fig. 1 A SEM cross-section view of the PEDOT:PSS/glass substrate

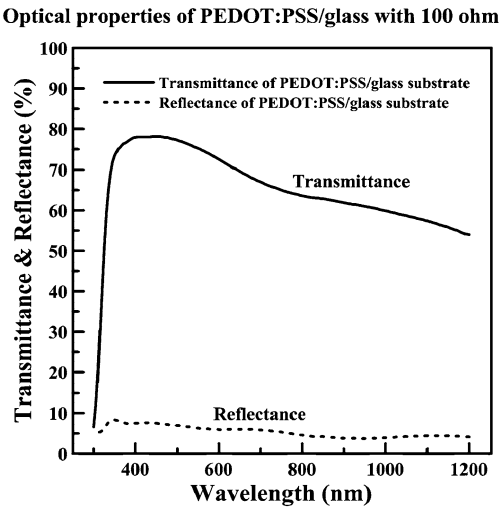

Fig. 2 Light transmittance and reflectance versus wavelength for the PEDOT:PSS/glass substrate

of the PEDOT:PSS film were 0.44 GPa and 8.21 GPa, respectively, measured by a nano-indentation instrument. The root mean square (RMS) roughness of the PEDOT:PSS films coated on the glass substrates was of 2.9 nm measured by an atomic force microscope (AFM, Veeco model Dimension 3100) with a measuring region of $1 \times 1\ \mu m^2$. After the laser patterning, the surface morphology was measured by a 3D laser confocal microscope (KEYENCE VK-9700).

2.3 Laser patterning parameters and electrode structures

Laser patterning parameters including the laser fluence, the scanning speed (V) of galvanometers, and the laser pulse repetition frequency (P_{RF}) could be adjusted to ablate out the PEDOT:PSS thin film deposited on glass substrates. Figure 3 outlines the schematic diagram of the laser spot overlaps and line scan spacing when the laser spot diameter (D)

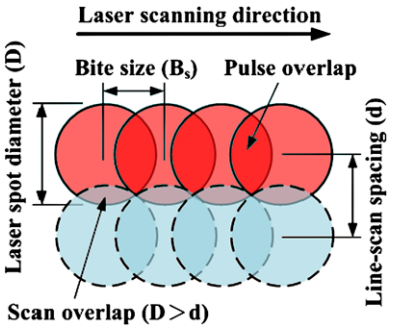

Fig. 3 Schematic outline of laser spot overlaps and line scan spacing

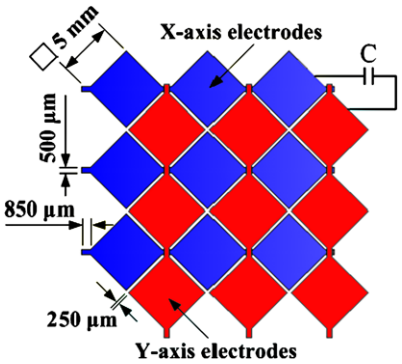

Fig. 4 Schematic diagram of the electrode structure for capacitive touch screen

is larger than line scan spacing (d). The overlapping rates (O_R) of laser spot is defined and calculated by the following equation [3]:

$$O_R = \frac{D - B_s}{D} \times 100\ \% \tag{1}$$

where B_s is the bite size between neighboring laser spots. The B_s value represents as

$$B_s = \frac{V}{P_{RF}} \tag{2}$$

The measured D value was approximately 30 µm. Moreover, the P_{RF} value was fixed at 50 kHz. According to the Eqs. (1) and (2), the designed patterns with 90 % O_R and the V value of 150 mm/s could be computed and obtained.

Figure 4 shows the electrode structure of capacitive touch screen where the blue and red areas are X- and Y-axis electrodes, respectively. The total dimension of glass substrates was 30 mm × 30 mm, and the area of patterned PEDOT:PSS thin film was 25 mm × 25 mm. The designed dimension of each rhombus was 5 mm wide and 5 mm long with a gap width of 250 µm between the neighboring isolated regions. Moreover, the dimension of each linear micro-pattern was 500 µm wide and 850 µm long.

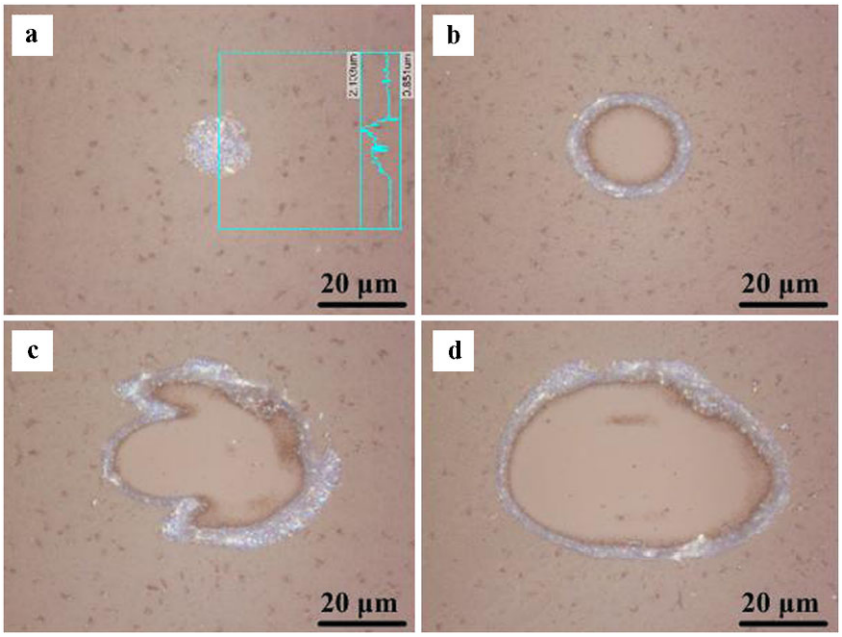

Fig. 5 Typical surface morphologies of interacted area between the single pulse laser and PEDOT: PSS film surface at laser fluences of 0.113 J/cm^2 (**a**), 0.283 J/cm^2 (**b**), 1.415 J/cm^2 (**c**), and 2.12 J/cm^2 (**d**), respectively

3 Results and discussion

3.1 Single-pulse laser induced ablation

The ablation threshold represents the minimal laser fluence demanded for the treated material to begin ablating. The ablation threshold is practically determined by ablated surface observation when the workpiece is ablated with various laser energies at a predetermined scan speed. The ablation threshold (F_{th}) could be estimated as the following equation [12]:

$$D^2 = 2\omega_0^2 \ln\left(\frac{F}{F_{\text{th}}}\right) \tag{3}$$

where D, ω_0, and F are the diameter of a crater ablated by a single pulse, the focused beam radius, and the incident peak fluence in J/cm^2, respectively. To clearly observe the ablated crater created by the single pulse, the UV laser beam was scanned along a line pattern with a scanning speed of 5000 mm/s and a pulse repetition frequency of 50 kHz. Hence, the center distance between neighboring craters could be calculated according to Eq. (2) and was approximately 100 μm along the patterned line.

Figure 5 shows a series of surface morphologies on the PEDOT:PSS film surface generated from the single pulse laser at laser fluences of 0.113 J/cm^2 (a), 0.283 J/cm^2 (b), 1.415 J/cm^2 (c), and 2.12 J/cm^2 (d), respectively. These images were taken by a 3D confocal laser scanning microscope with 3000 times magnification. The measured and observed results revealed that the interacted crater region increased with increasing the laser fluence. When the laser fluence was 0.113 J/cm^2, the region was bulged about 150 nm in height but no ablating was observed at the film, as shown in Fig. 5(a). When the incident laser fluence is less than the ablation threshold, the heated polymer film does not produce a physical ablation phenomenon after the laser irradiation. When the laser fluence increased from 0.283 J/cm^2 to 2.12 J/cm^2, the interacted region on the film surface was ablated out and the melted edge was curled to pile up around the hole to form a crater, as shown in Fig. 5(b) to (d), respectively. The hole shapes were irregular circles, as shown in Figs. 5(c) and (d), and the single laser pulse clearly damaged the glass substrate, indicated by arrow, at laser fluence of 2.12 J/cm^2. Moreover, the melted area and the curled height of the pile-up increase with increasing the laser fluence. This phenomenon was attributed to the photomechanical or stress-assisted ablation for the polymer film that could

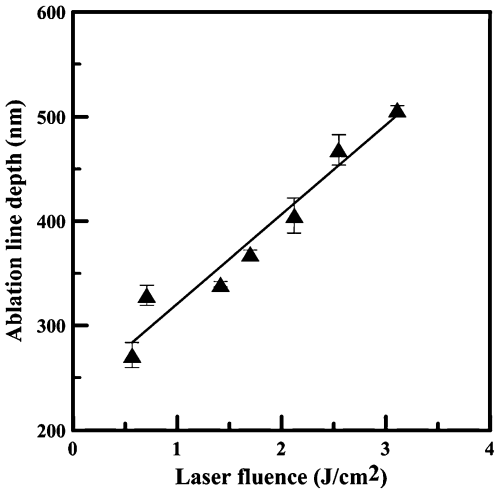

Fig. 6 Relationship of ablated line depths versus the various laser fluences

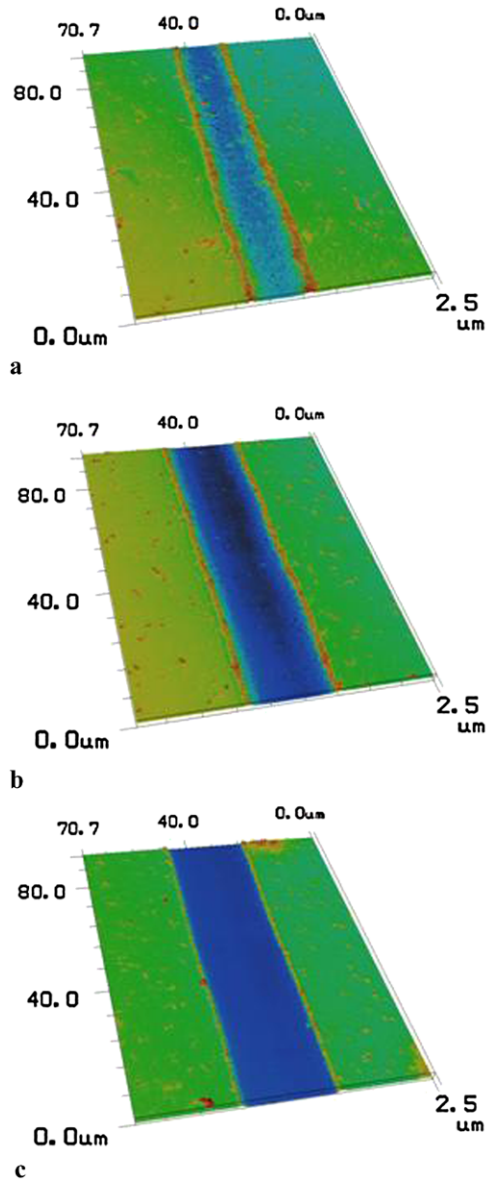

Fig. 7 Typical 3D topographies of laser patterning lines with different laser fluences on PEDOT:PSS/glass substrates: (**a**) 0.566 J/cm^2, (**b**) 0.708 J/cm^2, and (**c**) 1.7 J/cm^2

cause weakening, mechanical fracture, and explosive ejection of the film from the substrate surface [13, 14]. According to Eq. (3) and the mentioned experiments above, the ablation threshold of the PEDOT:PSS film conducted by the nano-second pulsed UV laser is 0.135 ± 0.003 J/cm^2.

3.2 Line patterning by laser ablation

The laser fluence was a major factor of laser patterning parameters, which strongly affected the width and depth of ablated lines. The designed ablation line patterns with 90 % O_R were executed with the laser pulse repetition frequency of 50 kHz and the scanning speed of 150 mm/s. Figure 6

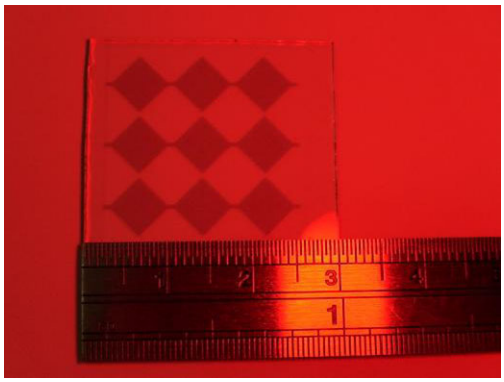

Fig. 8 A picture of electrode structures fabricated with the laser fluence of 1.7 J/cm^2 and 90 % overlapping rate on the PEDOT:PSS/glass substrate

shows a relationship of ablated line depths versus the various laser fluences. The experimental results showed that the ablated line depth increased linearly with increasing laser fluence. When the laser fluences were 0.566 J/cm^2 and 0.708 J/cm^2, the corresponding ablated depths were 272 ± 12 nm and 329 ± 9 nm, respectively. Because the thickness of PEDOT:PSS film was 330 nm, the ablated film along a patterned line path was incompletely removed. When the laser fluences were 1.415 J/cm^2 and 1.7 J/cm^2, the ablated line depths were 340 ± 3 nm and 368 ± 4 nm, respectively. The fluence intensities within these ranges were enough to remove the film completely without damaging the glass substrate. When the laser fluence increased from 2.12 J/cm^2 to 3.11 J/cm^2, the ablated line depths increased from 405 ± 16 nm to 507 ± 4 nm. The fluence intensities were too strong and caused damages in the glass substrate.

Figure 7 shows the typical 3D topographies of ablated lines on PEDOT:PSS/glass surface for various laser fluences examined under the 3000× magnification. The measured results of ablated lines showed that the inner line widths increased with increasing the laser fluence but the shoulder widths increased with fluence decrease, respectively. The polymer film was unevenly removed and resulted in crater height increase and high piled-up shoulder along the patterned edges when the laser fluence was 0.566 J/cm^2, as shown in Fig. 7(a). The inner line width and shoulder width of ablated PEDOT:PSS films were averagely 12.8 μm and 3.45 μm, respectively. When the laser fluence increased to 0.708 J/cm^2, the inner line width and shoulder width of line edges in Fig. 7(b) were averagely 17.57 μm and 1.81 μm, respectively. The ablated surface along the patterned line in Fig. 7(b) was more uniform compared with Fig. 7(a); however, few of film debris along the patterned line path were remained and seen clearly in these figures. A clean, smooth, and straight ablated groove was observed as shown in the blue line of Fig. 7(c), and no PEDOT:PSS debris was left in the line or around neighboring bank after the line patterning was conducted with the laser fluence of 1.7 J/cm^2. The

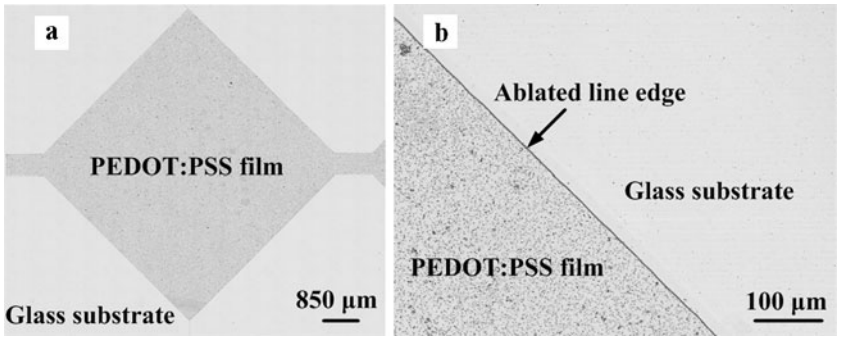

Fig. 9 Photographs of (**a**) the electrode assembled by 238 pieces of assembled blocks and (**b**) enlarged a partial electrode measured by the 3D laser confocal microscope

inner line width and shoulder width of patterned line edges in Fig. 7(c) were averagely 20.91 μm and 0.86 μm, respectively.

3.3 Patterning electrode structures for touch screens

Based on ablated lines results discussed above, the laser fluence of 1.7 J/cm^2 combined with 90 % overlapping rate was preferable to obtain a good ablation quality of the patterned edged electrode profile. Therefore, these processing parameters were selected to fabricate the partial X- and Y-axis electrode structure of touch screens in this study. The laser patterning paths were parallel lines with equal line scan spacing. The dimensions of scan area and line scan spacing (d) were 30 mm × 30 mm and 1 μm, respectively. After the laser patterning of electrode structures for the touch screen was finished, the photo picture and surface morphology of electrode structures were taken by a digital camera with red lights and the 3D laser confocal microscope as shown in Figs. 8 and 9, respectively. The dark area was the un-ablated region in the PEDOT:PSS film, and the light area was the laser ablated region, shown in Fig. 8. The surface morphology of the electrode structure was measured using image assembly techniques, and Fig. 9(a) was constructed by 238 pieces of assembly blocks. The dimension of each assembly block was 500 μm × 703 μm. The measured results obviously revealed that the ablated region of PEDOT:PSS films had straight lines and sharp corners around the patterning boundaries. The boundary between the dark and light areas was clearly distinguishable, which implied the laser-ablated process was conducted smoothly and uniformly. Figure 9(b) showed the enlarged photo of a partial electrode on PEDOT:PSS/glass substrates examined under the 400× magnification. The ablated patterns had straight edges. Moreover, there was no significant heat affected zone produced near the patterned edges and no ablated debris remained or piled-up onto the surface of PEDOT:PSS films.

4 Conclusion

A nano-second pulsed UV laser system has been proposed to pattern the electrode structures on the PEDOT:PSS film. After the single pulse laser irradiation, the ablation threshold of the PEDOT:PSS film with a thickness of 330 nm was 0.135 ± 0.003 J/cm^2. The ablated region and the line depth under the interaction between single laser pulse and PEDOT:PSS film increased linearly with increasing the laser fluence. When the laser fluence increased from 0.566 J/cm^2 to 3.11 J/cm^2, the corresponding ablated depths were 272 ± 12 nm and 507 ± 4 nm, respectively. When the laser fluence increased from 0.566 J/cm^2 to 0.708 J/cm^2, the inner line width and shoulder width of line edges were averagely from 12.8 μm to 20.91 μm and 3.45 μm to 0.86 μm, respectively. Moreover, the clean, smooth, narrow, and straight ablated groove without PEDOT:PSS debris in the patterned line or around neighboring bank was obtained after the line patterning with the laser fluence of 1.7 J/cm^2 and 90 % overlapping rate. The ablated electrode had straight edges and sharp corners. Therefore, the electrode patterning on PEDOT:PSS thin films is accomplished by the proposed UV laser processing system.

Acknowledgements The authors thank the National Science Council of Taiwan for financially supporting this research under contract nos. NSC 100-2622-E-492-002-CC3 and NSC 99-2221-E-492-014, and measuring supports from Nano/MEMS and precision machining shops of the Instrument Technology Research Center, Taiwan, are also acknowledged.

References

1. O.A. Ghandour, D. Constantinide, R. Sheets, Proc. SPIE Int. Soc. Opt. Eng. **4637**, 90 (2002)
2. S.F. Tseng, W.T. Hsiao, K.C. Huang, D. Chiang, M.F. Chen, C.P. Chou, Appl. Surf. Sci. **257**, 1487 (2010)
3. S.F. Tseng, W.T. Hsiao, K.C. Huang, D. Chiang, Appl. Surf. Sci. **257**, 8813 (2011)
4. H.J. Booth, Thin Solid Films **453**, 450 (2004)
5. H. Yu, H. Lee, J. Lee, H. Shin, M. Lee, Microelectron. Eng. **88**, 6 (2011)
6. M.F. Chen, W.T. Hsiao, Y.S. Ho, S.F. Tseng, Y.P. Chen, Thin Solid Films **518**, 1072 (2009)

7. T. Roch, E. Beyer, A. Lasagni, Diam. Relat. Mater. **19**, 1472 (2010)
8. H. Shin, H. Yoo, M. Lee, Appl. Surf. Sci. **256**, 2944 (2010)
9. H.K. Lin, C.H. Li, S.H. Liu, Opt. Lasers Eng. **48**, 1008 (2010)
10. C.J. Hayden, C. Dalton, Appl. Surf. Sci. **256**, 3761 (2010)
11. P.-O. Westin, U. Zimmermann, M. Edoff, Sol. Energy Mater. Sol. Cells **92**, 1230 (2008)
12. J.M. Liu, Opt. Lett. **7**, 196 (1982)
13. G. Paltauf, P.E. Dyer, Chem. Rev. **103**, 487 (2003)
14. N.G. Semaltianos, C. Koidis, C. Pitsalidis, P. Karagiannidis, S. Logothetids, W. Perrie, D. Liu, S.P. Edwardson, E. Fearon, R.J. Potter, G. Dearden, K.G. Watkins, Synth. Met. **161**, 431 (2011)